JOURNAL OF MATERIALS SCIENCE 27 (1992) 2165–2172

Crystallization of fibres inside a matrix: a new way of fabrication of composites

S. T. MILEIKO, V. I. KAZMIN†
Solid State Physics Institute of the Academy of Sciences of the USSR, Chernogolovka Moscow district 142432, USSR

Fibrous composites are normally fabricated by inserting premade fibres into a matrix and trying to tailor mechanical or physical properties of the material by a proper choice of fibre arrangement, fibre volume fraction, structure and properties of interface, etc. As a rule, this method satisfies all the needs fairly well. But in many cases, particularly when heat-resistant composites are involved, it leads to complications which cause composite experts to refrain from being involved in technically very attractive projects. So the need for alternative methods of composite fabrication obviously exists. The process described here is an example of such an alternative. It is based on the fibres growing from the melt within the volume of the matrix. The matrix should have prefabricated continuous cylindrical channels to be filled with the melt of the fibre material. The process is described using as a model a composite with a molybdenum matrix and single crystalline sapphire fibres. It is shown that the productivity of oxide fibre fabrication based on the process described can be some orders of magnitude higher than that based on the well known Czochralsky's and Stepanov's methods. The strength of the single-crystalline sapphire fibres obtained has been studied, as well as the high-temperature creep strength of composites containing such fibres. Some of the results of these experiments are reported here.

1. Introduction

Fibrous composites are normally fabricated by incorporating premade fibres into a matrix and trying to tailor the mechanical or physical properties of the material by a proper choice of fibre arrangement, fibre volume fraction, structure and properties of interface, etc. As a rule, such a method satisfies all the requirements fairly well, but in many cases it leads to complications which restrict the involvement of them in technically very attractive projects. At least two examples can be given. The first, which has been known for some time, involves single-crystalline alumina fibres [1]. Such fibres are characterized by quite high strength values at elevated temperatures, but have still not been used, most certainly because of too high a fabrication price. The second example is more recent: the reports of the involvement of whiskers in the contraction of cancer is now well known, and has been widely discussed. Therefore the need for alternative methods of composite fabrication does obviously exist. A process described in the present paper is one example of an alternative method, called the method of internal crystallization (MIC), in which the fibres are grown from the melt within the volume of the matrix. The matrix should have prefabricated continuous cylindrical pores which are filled with the melt of the fibre material. The method will be described using as a model a composite with a molybdenum matrix and sapphire fibres.

2. Fabrication of Al_2O_3–Mo composites

The method of internal crystallization consists of three steps: (i) the formation of continuous cylindrical pores in the matrix; (ii) the infiltration of the pores with the melt of a fibre material; (iii) growth of fibres by crystallization of the melt. Obviously, the second and the third steps can be performed if the melting temperature of the fibre is lower than the melting temperature of the matrix, and chemical interaction between the matrix material and the melt is negligible. It is very convenient to have a good wetting of the matrix with the melt of fibre substance. All these demands are satisfied in the case of a sapphire–molybdenum composite. In fact, the melting temperatures of matrix and fibre materials are 2610 and 2070 °C, respectively, and the wetting angle is about 15° at 2100 °C. Little chemical interaction can be observed at the melting point of the fibre.

The first step of the fabrication process is the formation of continuous cylindrical pores in the matrix. This can be easily achieved in a metal matrix, using the procedure described below. First a layered assembly of foils and wires, of the same material, is prepared as shown in Fig. 1a. Then the assembly is subjected to diffusion bonding (Fig. 1b) under appropriate temperature – pressure – time conditions to provide a strong enough bond between the foils and the wires, but also to prevent the gaps between the neighbouring wires from being filled with the solid material. This yields a

0022–2461

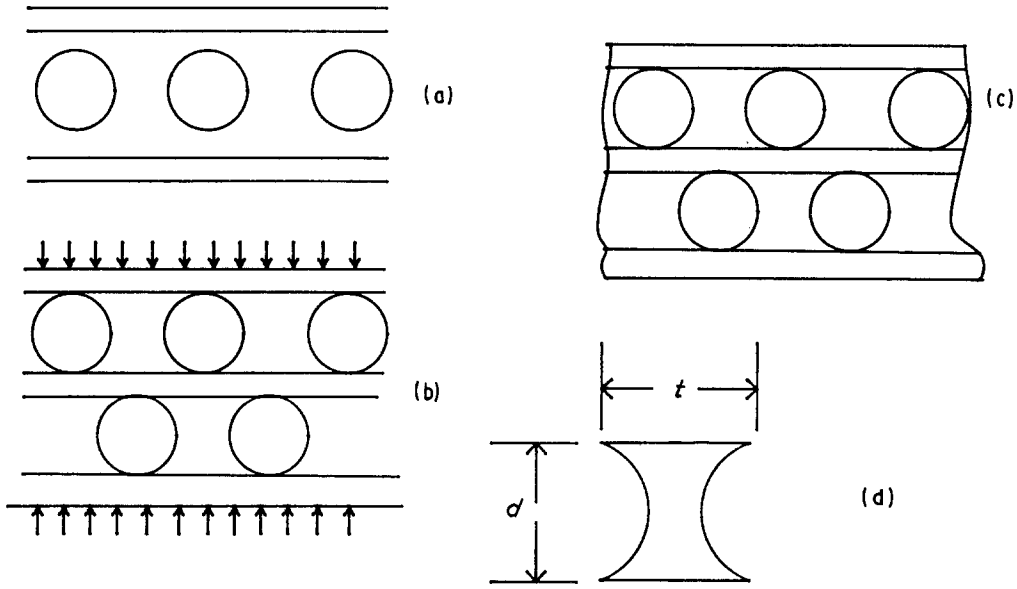

Figure 1 The fabrication steps of a metal matrix: (a) assembling the foil and wire layers; (b) diffusion bonding, and the final shape of the matrix with (c) channels and (d) the fibre cross-section.

structure, shown in Fig. 1c, which has continuous cylindrical pores. The shape of the transverse section of a single pore is shown in Fig. 1d; that will be the shape of a future fibre. The particular set of diffusion bonding conditions depends on the matrix material and the geometry. The temperature can be fixed for a particular matrix material, being equal to 1200 °C for molybdenum. It is clear that a particular composite part can be shaped easily before infiltration. For example, a specimen for a tensile test is made using an electric spark machine. The length of a constant cross-sectional part of the specimen used in the present work was 20 mm, the size of the cross-section was 1–2 × 5 mm.

The second step is the infiltration of the melt into the cylindrical pores in the matrix. If wetting occurs, this step is self-governing when a piece of the matrix contacts the melt. The temperature of the Al_2O_3 melt should be about 2200 °C.

The final step is crystallization of the fibres in the pores. Let us initially consider qualitatively a possible model of the crystallization process. Suppose we have a furnace with two temperature zones I and II (Fig. 2) and there is no direct thermal exchange between them. Immediately after the infiltration, the specimen is located within Zone I and its temperature is T_i which is higher than the melting temperature T_m of the matrix. Now if the specimen is moved instantaneously in the direction of the arrow (Fig. 2) by ΔL, the temperature profile along the specimen starts to change, as shown by lines marked with $t = 0, t_1, t_2, \ldots$.

To initiate crystallization it is necessary to have some value of overcooling, say ΔT. So at some time, say t_3, the temperature at the right-hand end of the specimen is $T_m - \Delta T$ and spontaneous crystallization within the length L^* occurs. There is no reason to observe any results of this process other than for the polycrystalline fibres within this part of the specimen, but it is important to note that as the pore effective diameter decreases, the probability of having a single

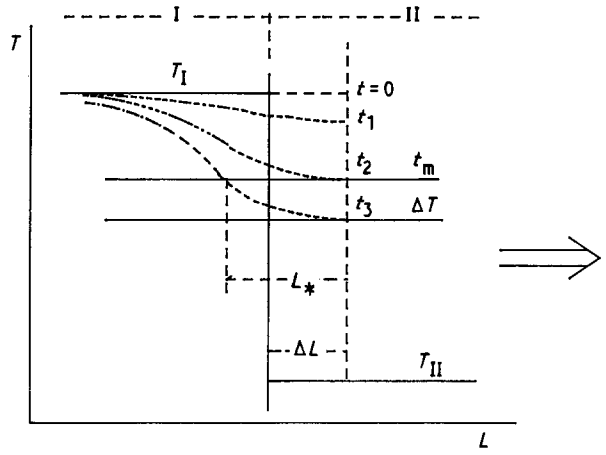

Figure 2 Schematic representation of temperature profiles in the crystallization zone.

crystal occupying the whole pore transverse section increases.

Now, if the specimen is moved from Zone I to Zone II at a definite rate, u, then, obviously, the length L^* of the specimen with spontaneously crystallized fibres depends on the value of u: the larger the rate the bigger is this length. After this initial stage of crystallization in a moving specimen, crystals at the left-hand boundary of the crystallized zone occur as seeds for fibres growing in pores. Thus the fibre can have single crystalline structure along the whole pore length to the left from the initial crystallization front.

A quantitive model of the process, which remains to be performed, should yield a critical effective diameter, d_{cr}, of the pore such that at a particular value of u single crystalline seeds should definitely appear.

3. Fibre structure

First, both poly- and single-crystalline parts of a fibre can be seen when looking at a layer of fibres extracted

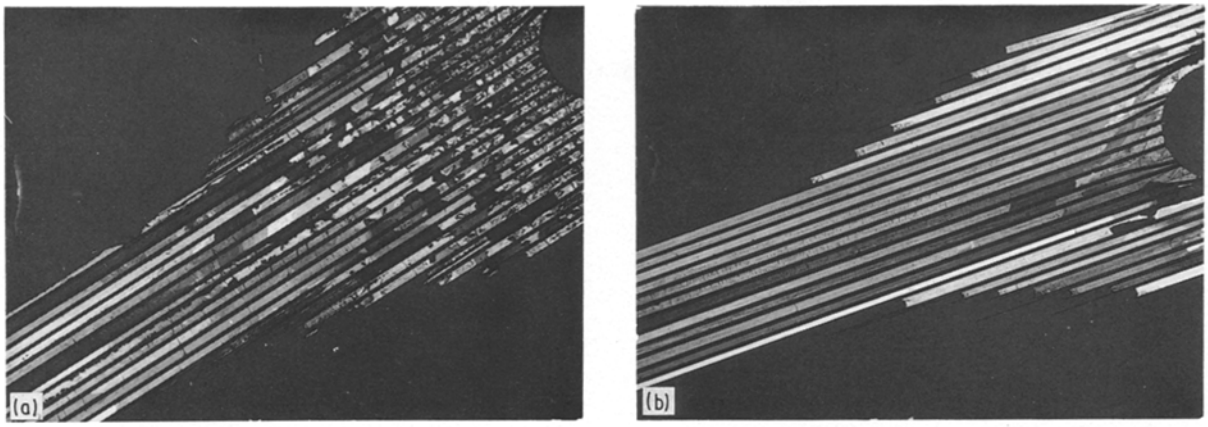

Figure 3 A layer of sapphire fibres photographed in polarized light, the polarization planes being perpendicular to each other. Molybdenum wires are located between the sapphire fibres. (a) Crystallization rate 15 mm min^{-1}, (b) Crystallization rate 7 mm min^{-1}.

from the matrix (Fig. 3). Note that optically anisotropic sapphire crystals, observed in a polariscope with crossed polarization planes, appear to be transparent only if the light beam direction does not coincide with the c-axis and the apparent colour is determined by the phase difference of two partial beams. The latter depends on both the crystal thickness and its orientation.

Therefore, the size of the polycrystalline part of a layer of the fibres increases when the pulling rate of a specimen increases.

Finally, it should be noted that the crystal orientation is not constant within a fibre layer. So a specimen with single crystalline fibres can be considered to be an effective polycrystal.

The angle, φ, between the c-axis of a hexagonal optically transparent crystal, e.g. sapphire, and the fibre axis, can be measured by observing fibre orientations with respect to the polarized light beam direction corresponding to the black appearance of the fibre. Such a procedure has been performed for ten specimens obtained under various conditions, with various fibre volume fractions and fibre sizes. 100 fibres were extracted from each specimen for the measurements.

Most of the histograms of φ are shown in Fig. 4. It can be seen that the values of φ lie mainly between 45° and 90°. It should be noted that no apparent dependence of the shape of a histogram on the parameters mentioned above has been observed.

4. Strength of composites and fibres

Before describing the experimental results, mention should be made that some experimental data have been published earlier [2, 3] without giving details of the fabrication procedure, as well as composite and fibre structure.

Now we begin by noting that variations of fibre volume fraction in the specimens fabricated by the present method are accompanied by variations in both characteristic sizes and proportions of the fibre cross-sectional shape, simply because of the normal restrictions for a choice of sets of foil thicknesses and wire diameters when producing the matrix. That must be taken into account when analysing the failure behaviour of the composites. To analyse this behaviour a micromechanical model of the strength of composites is also required. We shall use here the model describing the failure of metal matrix/brittle fibre composites published earlier (see, for example, [3, 4]).

At low enough fibre volume fractions, v_f, when the failure process of a composite is developing by accumulation of non-interactive fibre breaks, composite strength, σ^*, depends on v_f as

$$\sigma^* = \alpha\langle\sigma_f^*(l^*)\rangle v_f + \sigma_m^*(1 - v_f) \quad (1)$$

where the value of σ_m^* can be taken as the matrix ultimate stress, l^* is the critical length, and α is a constant of the order of 1.

The equilibrium of a fibre loaded up to failure by shear stresses, τ^*, distributed on its surface (τ^* is either the interface strength or the yield stress of the matrix in the vicinity of the interface) yields

$$\langle\sigma_f^*(l^*)\rangle/\tau^* = sl^*/4F \quad (2a)$$

or

$$\langle\sigma_f^*(l^*)\rangle = \tau^*\frac{l^*p}{df} \quad (2b)$$

where $p = 2t/d + \pi$, $f = 4t/d - \pi$, s and F are the perimeter and the area of the fibre cross-section, respectively.

On the other hand, there exists a scale dependence of the fibre strength which certainly is of the Weibull's type but *a priori* it is not clear what should be the dimension of the scale. Because there is a variation in the fibre cross-section with the variation of fibre volume fraction, the dimension can be either the length or the surface or, finally, the volume. All three hypothesies and an experiment will be investigated. Let us write the scale dependence as

$$\langle\sigma_f^*(l^*)\rangle = \sigma_0(k_\mu^0/k_\mu^*)^{1/\beta} \quad (3)$$

where $\mu = 1, 2, 3$, and $k_1^* = l^*$, $k_2^* = l^*pd$, $k_3^* = 0.25\,l^*fd^2$ correspond to the particular hypotheses. The same is true for constants $\sigma_0(k_\mu^0)^{1/\beta} = A_\mu$. A particular value of A_μ as well as β depends upon μ.

Comparing Equations 2 and 3 and excluding the value of l^*, which is not measured in direct mechanical

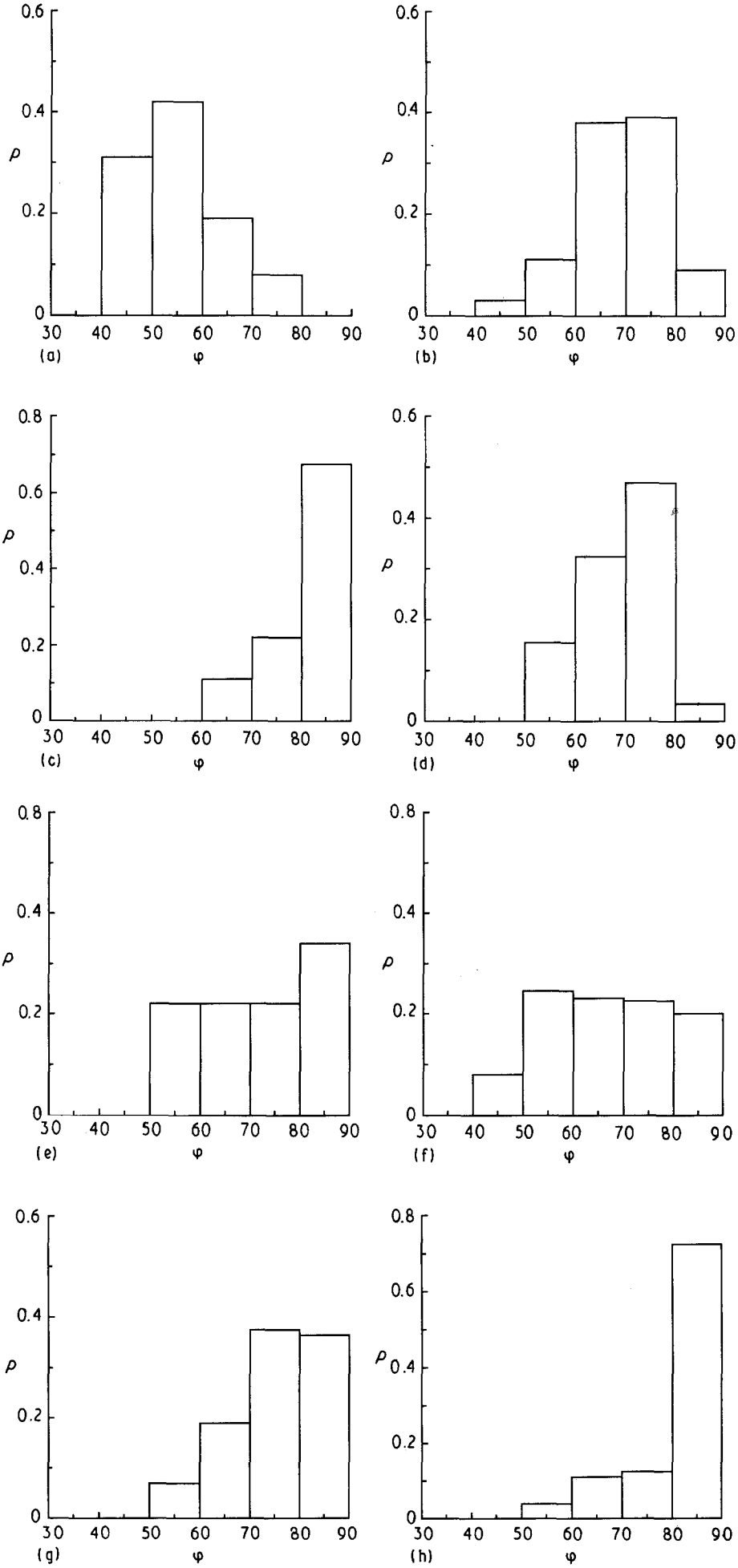

Figure 4 Histograms of angles between the *c*-axis of the sapphire crystal and the fibre axis. The diameter of molybdenum wire, 50 μm; pulling rate 7 mm min^{-1}. Fibre volume fraction: (a–d) 0.17, (e, f) 0.33, (g, h) 0.46.

tests, we obtain

$$\langle \sigma_f^*(l^*) \rangle = B_\mu \lambda_\mu^{1/(1+\beta)} \quad (4)$$

where

$$B_\mu = A_\mu^{\beta/(1+\beta)} (\tau^*)^{1/(1+\beta)}$$

if $\mu = 1, 2,$

$$B_3 = A_3^{\beta/(1+\beta)} (4\tau^*)^{1/(1+\beta)}$$

$\lambda_1 = p/fd, \lambda_2 = 1/fd^2, \lambda_3 = p/f^2d^3$. Therefore Equation 1 can be rewritten as

$$\sigma^* = (\alpha B_\mu \lambda_m^{1/(1+\beta)} - \sigma_m^*) v_f + \sigma_m^* \quad (5)$$

and finally as

$$S^* = C_\mu \lambda_\mu^{1/(1+\beta)} \quad (6)$$

where $C_\mu = \alpha B_\mu, S^* = \sigma_m^* + (\sigma^* - \sigma_m^*)/v_f$

The dependences given by Equation 6 are shown in Fig. 5. Approximating the experimental dependences by power functions, we obtain the values of β and C_μ given in Table I. Obviously the value of β, obtained for the linear scale in Equation 3 is non-admittable, but there are no strict grounds to choose a proper value of β between those for $\mu = 2$ and $\mu = 3$. Still the value for the "volume" hypothesis ($\beta = 3.24$) looks more realistic.

This conclusion is confirmed by observations of fracture surfaces of fibres. An example of a typical surface shown in Fig. 6 illustrates a usual defect which initiates the fracture. Such voids are distributed within the volume of a fibre. One reason for their occurrence is a shortage of the melt near the crystallization front because of the volume effect at crystallization. This leads to a demand to decrease the pulling rate, u, at

TABLE I Statistical strength characteristics of sapphire fibres in a molybdenum matrix

μ	β	C_μ (MPa)
1	0.350	41.8
2	1.82	98.6
3	3.24	73.6

composite fabrication. Experiments [5] point to a value $u = 7$ mm min^{-1} as a reasonable upper limit. This also satisfies a demand to have a small enough size of the polycrystalline region in a specimen.

It should be noted that fibre breakage in a composite during loading is not equivalent to cutting a fibre at arbitrary points. The process in a composite continues through weak points along a fibre which amplifies the scale effect. So the data obtained must be applied to estimation of the scale effect for fibres in the matrix when the composite failure is a result of fibres-break accumulation.

At the other extreme of composite failure mechanisms, is the failure of a specimen immediately after a first fibre break at a weakest point. It usually involves quite a large total fibre length, of the order of metres. It should be of some interest to evaluate β for this case. Let us do this by assuming the "volume" hypothesis is true. If the total fibre length in a specimen with a fixed number of layers and a constant length of its homogenous part is $L = nb/t$, then Equation 3 can be rewritten as

$$\sigma_f^*(L) = C\lambda^{-1/\beta} \quad (7)$$

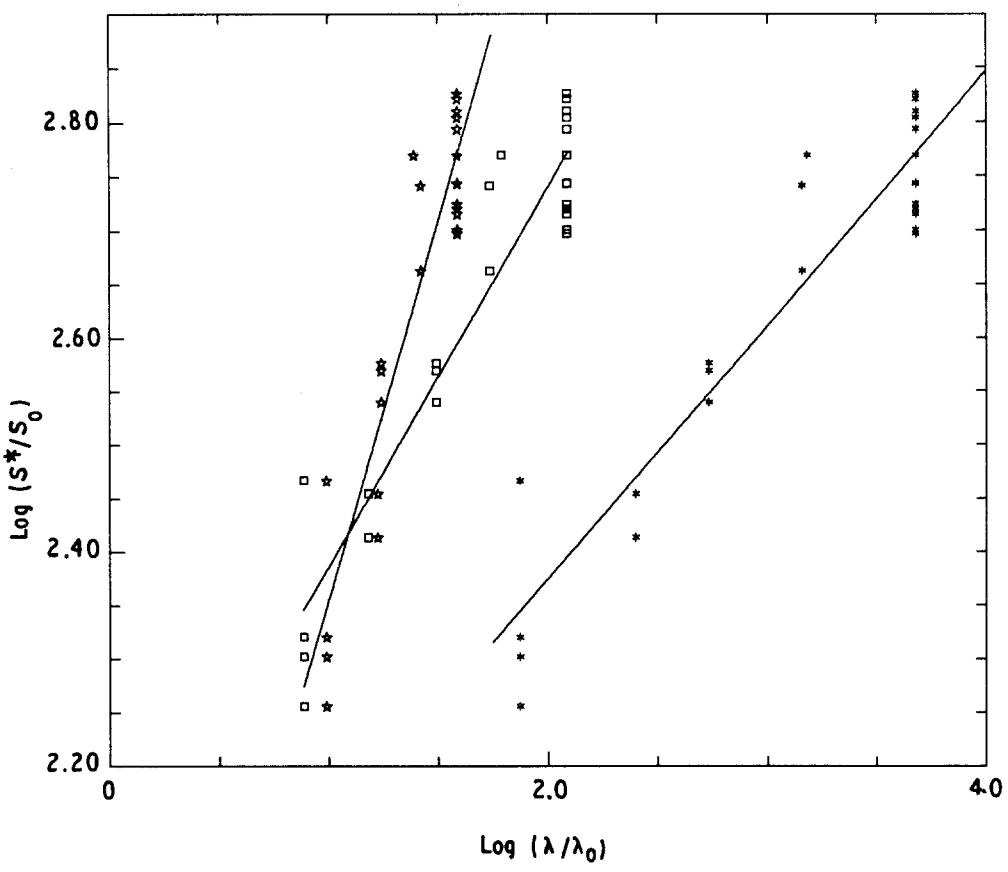

Figure 5 Determination of the scale dependence of the strength of a sapphire fibre in a molybdenum matrix at 1300 °C according to Equation 6. Logarithmic plot, $S_0 = 1$ MPa, (☆) $\lambda = 1$ mm^{-1} for $\mu = 1$, (□) $\lambda = 1$ mm^{-2} for $\mu = 2$, (*) $\lambda = 1$ mm^{-3} for $\mu = 3$.

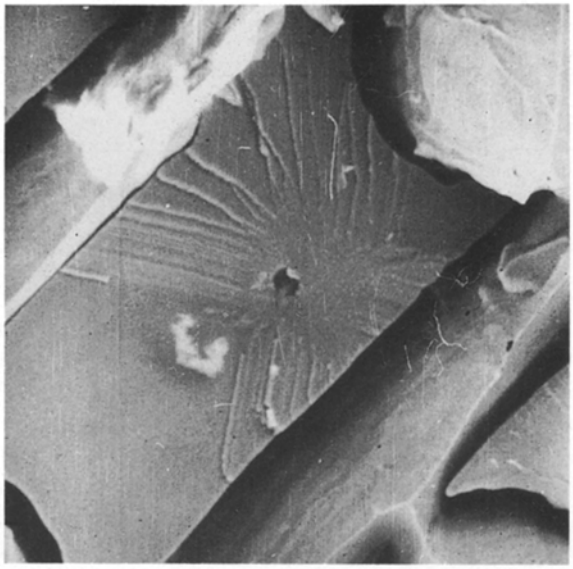

Figure 6 Failure surface of a sapphire fibre. The pore, certainly initiating the failure, can be seen.

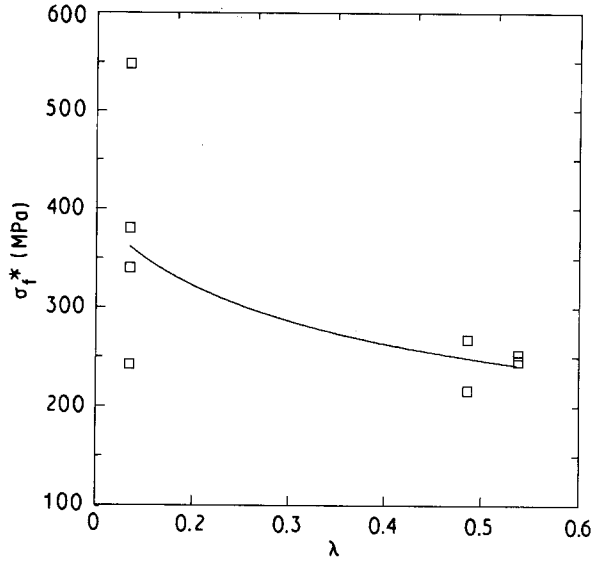

Figure 7 Determination of the scale dependence of the strength of a sapphire fibre for fibre lengths of the order of metres at 1300 °C according to Equation 7.

TABLE II Results of tensile tests at 1300 °C of Mo–Al_2O_3 composites obtained at a crystallization rate of 7 mm min^{-1}

NN	d (mm)	δ (mm)	t (mm)	σ* (MPa)	v_f
4882	0.2	0.1	0.32	110	0.34
4885	0.20	0.10	0.32	142	0.34
4883*	0.20	0.10	0.40	129	0.40
4884*	0.20	0.10	0.40	108	0.40
5849	0.20	0.10	0.32	113	0.34
5380*	0.20	0.10	0.48	132	0.45
5511*	0.20	0.10	0.48	129	0.45
5240	0.078	0.04	0.12	192	0.32
5297	0.078	0.04	0.12	222	0.32
7240	0.05	0.03	0.08	250	0.32
7241	0.05	0.03	0.08	215	0.32
7243	0.05	0.03	0.08	245	0.32
7292*	0.05	0.03	0.12	164	0.42
7297*	0.05	0.03	0.12	122	0.42
7481	0.05	0.10	0.08	163	0.17
7483	0.05	0.10	0.08	166	0.17
7489	0.05	0.10	0.08	142	0.17
7617	0.05	0.10	0.08	141	0.17
7618	0.05	0.10	0.08	147	0.17
7619	0.05	0.10	0.08	138	0.17
7500*	0.05	0.03	0.12	253	0.42
7629	0.05	0.03	0.08	261	0.32
7630	0.05	0.03	0.08	223	0.32
7901	0.05	0.03	0.08	234	0.32
8299	0.05	0.10	0.12	180	0.22
8556[a]	0.05	0.10	0.12	155	0.22
8560	0.05	0.20	0.20	108	0.16
8562	0.05	0.20	0.20	113	0.16
8563	0.05	0.20	0.20	112	0.16
7359*	0.05	0.03	0.12	181	0.42
8564	0.05	0.20	0.08	106	0.10
4881	0.20	0.10	0.32	103	0.34
5235	0.20	0.10	0.24	108	0.23
5234	0.20	0.10	0.24	114	0.23

[a] Multiple fibre breakage during cooling of the specimen.

where C is a constant, $\lambda = fd^2/t$, λ is introduced through λ_3. Now we use the values of composite strength measured in the tests again conducted at 1300 °C. Consider now only those specimens in Table II which are marked with an asterisk, which have failed in a fashion appropriate to this consideration. To calculate $v_f^*(L)$ the thermal stresses evaluated according to following relationship must be taken into account

$$\sigma_f^0 = E\Delta\alpha\Delta T/(1 + v_f/v_m) \quad (8)$$

where $E = E_f \approx E_m$ (a case when the components' moduli are nearly the same), $\Delta\alpha$ is the difference of linear expansion coefficients of the fibre and the matrix and $\Delta T = 1400$ °C for the reasons discussed previously [6]. Now the experimental data presented in Fig. 7 in accordance with Equation 7 lead to $\beta = 3.45$. The difference between this value and the value of β obtained for the short-lengths basis of the same fibres ($\beta = 3.24$) is, obviously, negligible.

It is important to note that the temperature dependencies of the fibres obtained by the MIC and those obtained by the well known Stepanov's method shown in Fig. 14 in Reference 3, display about the same level of the strength of all sapphire fibres.

5. Creep and creep–rupture

All the details of the creep tests of the composites are discussed elsewhere [5, 7], so here we only need highlight the accuracy of the measurements as follows. The values of the load were measured during the creep process to better than ±3 MPa (corresponding to ±3%). The temperature measurements (1300–1700 °C) had an accuracy of ±8 °C, and the maximum absolute error in the observation of specimen strain was 0.07%.

The creep properties of the composites at 1300 and 1700 °C differ qualitatively, so they will be considered separately.

Typical creep curves at 1300 °C of the composite with fibre effective diameter 200 μm are shown in Fig. 8. The creep characteristics of the matrix (the matrix being a specimen prepared for melt infiltration and undergone thermal treatment at 2100 °C) have been determined in a special experiment. In the power

creep law for the matrix expressed

$$\varepsilon = \varepsilon_m(\sigma/\sigma_m)^m \quad (9)$$

one can assume $m = 6$, $\sigma_m = 16$ MPa, $\varepsilon_m = 10^{-4}\,h^{-1}$

Fibre stress $\sigma'(t)$, normalized by the value of fibre stress σ_0/v_f at $t \to \infty$, increases as [8]

$$[\sigma'(t)/\sigma_0]v_f = 1 - (v_m)\{v/[v^m + \varepsilon_m(m-1)(v_f E_m/\sigma_m)(\sigma_0/\sigma_m)^{m-1}t]\}^{1/(m-1)} \quad (10)$$

where $v = v_m + v_f E_f/E_m$

Curves $[\sigma'(t)/\sigma_0]v_f$ for Mo–Al_2O_3 composites analysed in [5] reveal a very quick stress redistribution indicating that the time of the first fibre break in a composite should vary in a very broad interval even if fibre strength scatter is not too large. The interval should become broader with increasing fibre volume fraction. Qualitatively these conclusions correspond to the experimental results shown in Fig. 8; creep–rupture data are given in Fig. 9.

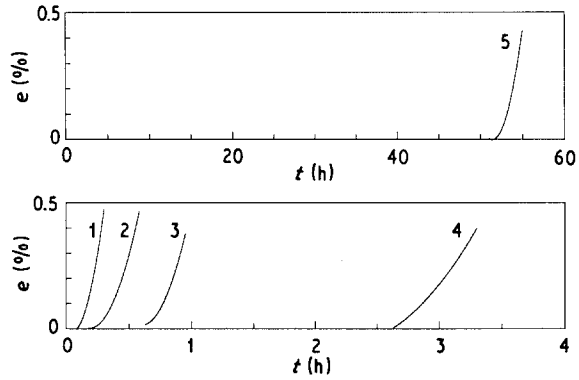

Figure 8 Creep curves of sapphire–molybdenum composites at 1300 °C. Fibre volume fractions are 0.40 (specimens 1, 3), 0.46 (2, 5), 0.33 (4).

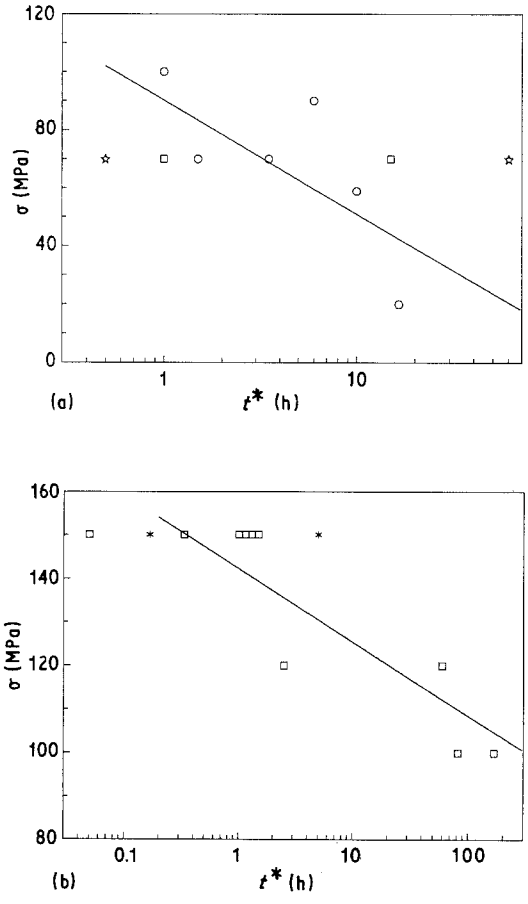

Figure 9 Creep strength of sapphire–molybdenum composites at 1300 °C. (a) $d = 200$ μm, $v_f = (\bigcirc)$ 0.33, $(\square)$ 0.40, $(\star)$ 0.46; (b) $d = 50$ μm, $v_f = (\square)$ 0.33, $(*)$ 0.46.

Here it should be noted that short-term tests of the composites with $v_f = 0.46$ and fibre diameter 200 μm at 1300 °C (Fig. 2a in Reference 2) indicate that composite failure occurs when the average fibre stress reaches 200–210 MPa. On the other hand, when a specimen creeps under the stress equal to 70 MPa (Fig. 8), the average fibre stress as a result of the pure stress redistribution without taking into account fibre creep, will be no more than 140 MPa. Creep–rupture time for this condition varies from 0.5–60 h, confirming the qualitative conclusion about a large scatter of rupture time.

In addition, this suggests that a stress redistribution between the fibres due to their various crystallographic orientation, is essential. The crystallographic orientation of part of the fibres is such that the basal plane of the sapphire crystal lies at an angle about 45° to the fibre axis. Such fibres creep easily, the stresses in these fibres decrease, and as a result well-oriented fibres take an extra load.

When the fibre diameter decreases to 50 μm then obviously the average strength of the fibre increases, leaving a general view of a composite failure process without essential changes. Nevertheless, a shift in fibre volume fractions should be noted for weakly interactive fibre breaks towards lower values (see for explanation [2]). The other important point is quite a large increase in creep–rupture stresses (Fig. 9b). However, the creep strength remains not high enough, the scatter is too large, and an increase in fibre volume fraction does not lead to an essential increase in creep strength.

In view of the clarity of the mechanism of creep failure, it becomes clear how to enhance the creep strength of composites of the type under consideration. It is necessary either to achieve a homogeneous fibre orientation which would be preferable from the view point of creep resistance, or to retard creep of fibres in some way. The first route can complicate the fabrication process. So the second one looks more worthwhile. This can be performed using eutectic mixtures of oxides as the fibre materials. It has been described in detail elsewhere [5, 7].

Typical creep curves of the composites at 1700 °C are presented in Fig. 10. The matrix creeps at this temperature according to power law given by Equation 1 with $m = 3.61$, $\sigma_m = 4.29$ MPa, $\varepsilon_m = 10^{-4}\,h^{-1}$.

The dependence of the creep rates of the matrix, the composites, and the fibres on the applied stress is shown in Fig. 11. The fibre stress during creep is

$$\sigma' = [\sigma - \sigma''(\varepsilon)]/v_f + \sigma''(\varepsilon) \quad (11)$$

where σ'' is the matrix stress determined through the

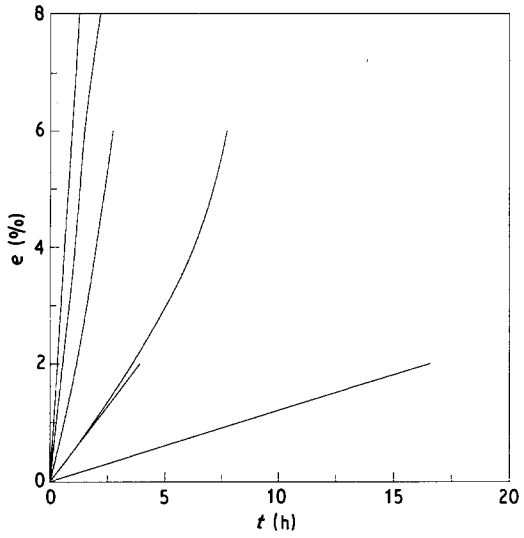

Figure 10 Creep curves of sapphire–molybdenum composites at 1700 °C, $\sigma = 30$ MPa.

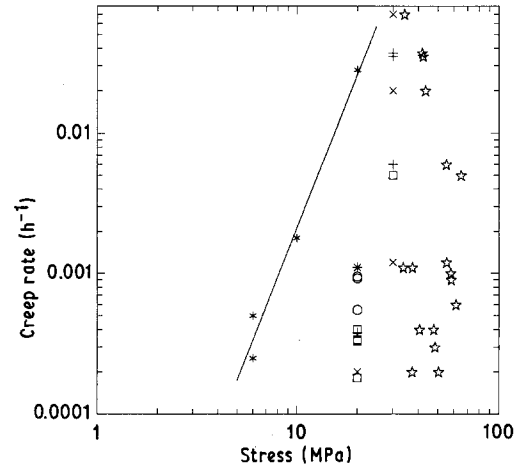

Figure 11 Stress dependences for creep rate of the matrix and sapphire–molybdenum composites. Calculated values of fibre stress at the stationary stage of creep of the composites are also shown in parentheses. Test temperature 1700 °C. v_f = (○) 0.24, (□) 0.33, (+) 0.40, (×) 0.46. (∗) Matrix, (☆) fibres.

creep rate, ε. Assuming all the fibres have the same crystallographic orientation, one obtains a dependence of creep rate of the fibre material on stress (Fig. 11) which is too strong (meaning $n \approx 40$ in creep law $\varepsilon = \varepsilon_n(\sigma/\sigma_n)^n$), if the points corresponding to the highest values of the creep rate are not taken into account. An obvious mistake appeared because of the poor approximation of creep behaviour of the matrix.

Such a value does not correlate with the data for the values of n previously obtained for sapphire crystals [9]. It appears that for the slip along the basal plane at 1550 °C, $n \simeq 4$. For a single crystal, when its c-axis deviates from a tension (compression) direction by 8°–10° within temperature interval 1200–1750 °C, $n = 19 \pm 4$. At the same time, experiments show [10] that the yield stress does strongly depend on temperature and crystallographic orientation. Therefore, for different orientations, the values of n and σ_n should be very different. The values of $n \simeq 40$ for sapphire fibres can be claimed to be too large for any orientation. Such values can be explained by assuming fibre orientations in the tested specimens have varied within a specimen as well as from specimen to specimen. Perhaps it may also explain the large scatter in creep rates of composites with a fixed fibre volume fraction.

6. Conclusions

1. The internal crystallization method can effectively be used for producing composites with single-crystalline fibres of refractory oxides.
2. The productivity of the oxide fibre fabrication processes based on the MIC can be some orders of magnitude higher than that based on the well-known Czokchralsky and Stepanov methods.
3. The effective strength of single-crystalline sapphire fibres obtained by the MIC is essentially the same as that for fibres obtained by traditional methods.
4. High-temperature creep strength of composites with continuous single-crystalline oxide fibres cannot be very high-enough because single-crystals are characterized by the existence of slip systems with low slip resistance.
5. A systematic study of the strength of Mo–Al_2O_3 composites supports the postulated efficiency of a model of composite failure.

Acknowledgement

One of the authors thanks Mr L. S. Kozhevnikov for his valuable help in the experiments.

References

1. H. E. LABELLE Jr and A. I. MLAVSKY, *Nature* **216** (1967) 574.
2. S. T. MILEIKO and V. I. KAZMIN, *Mech. Compos. Mater.* **4** (1979) 723 (in Russian).
3. S. T. MILEIKO, in "Strong Fibres", edited by W. W. Watt and B. V. Perov (North-Holland, Amsterdam, 1985) pp. 87–114.
4. S. T. MILEIKO, in "Fabrication of Composites", edited by A. Kelly and S. T. Mileiko (North-Holland, Amsterdam, 1983) pp. 221–94.
5. S. T. MILEIKO and V. I. KAZMIN, *Mecanica compozitnych materialov*, in press (in Russian).
6. V. I. KAZMIN, S. T. MILEIKO and V. V. TVARDOVSKY, *Compos. Sci. Technol.* **38** (1990) 69.
7. S. T. MILEIKO and V. I. KAZMIN, *ibid.*, in press.
8. S. T. MILEIKO, in "Mechanics of deformable solids and structures", edited by V. V. Novozhilov (Nauka, Moscow, 1975) pp. 294–7 (in Russian).
9. D. J. GOOCH and G. W. GROVES, *Phil. Mag.* **28** (1973) 623.
10. R. CHANG, *J. Appl. Phys.* **131** (1960) 484.

Received 7 January
and accepted 13 May 1991